

Transport properties of a molecular quantum dot coupled to one-dimensional correlated electrons

S. Maier¹ and A. Komnik¹

¹*Institut für Theoretische Physik, Ruprecht-Karls-Universität Heidelberg,
Philosophenweg 19, D-69120 Heidelberg, Germany*

(Dated: August 30, 2018)

We analyze the transport properties of a quantum dot with a harmonic degree of freedom (Holstein phonon) coupled to interacting one-dimensional metallic leads. Using Tomonaga-Luttinger model to describe the interacting leads we construct the generating function of the full counting statistics (FCS) for a specific constellation of system parameters and give explicit expression for the cumulant generating function. In the resonant case we find the lowest order correction to the current to be negative and divergent when source-drain voltage approaches the phonon frequency. Via a diagram resummation procedure we show, that this divergency can be repealed. On the contrary, in the off-resonant case the lowest order correction remains finite. This effect can be traced back to the strongly non-monotonic behaviour of the bare transmission coefficient (without phonon) with respect to the dot level energy. We calculate corrections to the noise power as well and discuss possible experimental implications of this phenomenon.

PACS numbers: 73.63.Kv, 72.10.Pm, 73.23.-b

Quantum impurities are often used to model ultrasmall quantum dots and contacted molecules. One of the most fundamental setups is the Anderson impurity model taking into account the local Coulomb interaction¹. Especially in the case of contacted molecules, however, an explicit consideration of coupling to vibrational degrees of freedom is also desirable. This is accomplished by the Anderson-Holstein model^{2,3}. Even under equilibrium conditions and in the absence of Coulomb repulsion it turns out to possess interesting properties. Recently a number of successful electron transport experiments carried out on contacted molecules revealed some very interesting details⁴⁻¹⁰. Probably the most prominent of them is the different behavior of the molecule conductance which can grow or decline as soon as the applied voltage gets larger than the phonon frequency.¹¹⁻¹⁷ This phenomenon can be understood as follows. At zero temperature and voltages the vibrational degrees of freedom can be safely assumed to be frozen out and one effectively deals with the (noninteracting) resonant level with some energy Δ . The spectral function of the quantum dot is a single Lorentzian with some width Γ (which is related to the hybridization of the dot level with the electrode) centered around Δ . For the large initial transmittance of the system Δ should lie in between the chemical potentials of the contacting electrodes. On the opposite, for small transmittance Δ is below/above the chemical potentials. The system is virtually insulating at $|\Delta| \gg \Gamma$ because then the spectral weight around the chemical potentials position, which is necessary for transmission, is very small. When the phonon gets excited its spectral function is known to develop equidistant sidebands^{18,19}. The central peak at Δ persists but due to spectral weight redistribution its height diminishes. Therefore the initially large transmission drops as soon as the vibrational degrees of freedom can be excited. On the contrary, due to the finite spectral weight in the sidebands the

conductance grows for the out-of-resonance Δ . It turns out that in general the crossover from enhanced to suppressed transmission does not correspond to any universal parameter constellation apart of the limiting cases of large/small Δ ^{11,12}. Nonetheless it has been observed in several experiments⁴⁻¹⁰.

Thus far only noninteracting electrodes were considered. Given the small dimensions of the corresponding devices it is very likely that the electrodes might in fact possess genuine one-dimensional geometry as far as the electronic degrees of freedom are concerned. Alternatively one might conceive a device contacted by e. g. armchair carbon nanotubes, which are known to host one-dimensional electrons. In these situations instead of conventional Fermi liquids one deals with the Tomonaga-Luttinger liquids (TLL). Their most prominent feature is the power-law singularity of the local density of states in vicinity of the Fermi edge. Among other things it results in complete suppression of transmission in presence of impurities in the low energy sectors leading to the zero bias anomaly (ZBA)^{20,21}. As a result the transmission through a featureless quantum dot coupled to two TLLs vanishes towards small voltages and low temperatures^{20,22-25}. The only exception is the perfect resonant setup when $\Delta = 0$ and hybridizations with both electrodes are equal to each other. Thus, contrary to the noninteracting electrodes, when the dot transmission can smoothly interpolate between perfect and zero transmission, in the TLL setup only two low-energy transmission regimes are possible: either zero or unity. Applying the above line of reasoning one might conclude that in the former case the current through the system starts to flow only after voltage gets larger than the phonon frequency. In the opposite case one would expect that the conductance of an initially perfectly transmitting dot would rapidly decrease beyond the threshold set by the phonon frequency. The goal of our paper is to under-

stand the details of transport properties of such a setup and to quantify this heuristic picture.

In order to proceed one needs a model which can equally good describe the off-resonant as well as perfectly transmitting case. While in the noninteracting case the resonant level model without phonon is trivially solvable this is not the case any more for the TLL with a generic interaction strength. Nonetheless, at one particular parameter constellation the problem is exactly solvable. We take advantage of this and analyze the transmission properties of the system with the phonon using the perturbation theory in the electron-phonon coupling. We model the system by the following Hamiltonian,

$$H = H_{\text{leads}} + H_{\text{dot}} + H_{\text{tunn}} + H_{\text{int}}. \quad (1)$$

H_{leads} describes two (R/L, right/left) metallic leads in the Luttinger liquid state kept at different chemical potentials $\mu_L - \mu_R = V$ with V being the bias voltage applied across the dot (we use units in which $e = \hbar = k_B = 1$ throughout), see for example Eqs. (2-4) of [30]. Since we are not interested in any spin or finite field related effects our dot Hamiltonian is given by

$$H_{\text{dot}} = \Delta d^\dagger d + \Omega c^\dagger c + g d^\dagger d (c^\dagger + c), \quad (2)$$

which describes a single fermionic level with energy Δ coupled with the amplitude g to the local oscillator with frequency Ω . d , d^\dagger and c , c^\dagger are the respective annihilation/creation operators for the electron and oscillator. H_{tunn} is responsible for the particle exchange between the electrodes and the dot,

$$H_{\text{tunn}} = \sum_{\alpha=R,L} \gamma_\alpha \psi_\alpha^\dagger(x=0)d + \text{H. c.} \quad (3)$$

where $\gamma_{R,L}$ are the (constant) tunneling amplitudes. The tunneling is assumed to be taking place locally at $x = 0$ in the coordinates of the respective electrode. The last term is the capacitive coupling of the electrodes to the dot

$$H_{\text{int}} = U_C d^\dagger d \left[\psi_L^\dagger(0)\psi_L(0) + \psi_R^\dagger(0)\psi_R(0) \right]. \quad (4)$$

The present problem allows for an exact solution for $g = 0$ and Tomonaga-Luttinger interaction parameter $K = 1/2$ while $U_C = 2\pi v_F$. The emergent structure is that of the Majorana resonant level model (MRLM) extended by the vibrational degree of freedom²⁶, in the case of the symmetric coupling $\gamma_L = \gamma_R = \gamma$

$$H = H_0[\xi, \eta] - i[\Delta + g(c^\dagger + c)]ab + i\gamma b\xi(0) + \Omega c^\dagger c. \quad (5)$$

The first part of the transformed Hamiltonian describes the electrodes in terms of new Majorana fermions ξ and η ,

$$H_0 = i \int dx \left[\eta(x)\partial_x\eta(x) + \xi(x)\partial_x\xi(x) + V\xi(x)\eta(x) \right]. \quad (6)$$

$a = (d^\dagger + d)/\sqrt{2}$ and $b = -i(d^\dagger - d)/\sqrt{2}$ are the respective Majorana operators for the dot fermion. In the absence of the phonon the transport properties of the above system are known even on the level of the full counting statistics (FCS)²⁷⁻²⁹. It is accomplished by introduction of the counting field λ into the Hamiltonian making it explicitly time-dependent due opposite signs of the counting field on the different Keldysh branches. In the model this is expressed in the replacement of the tunnel Hamiltonian $H_T = -i\sqrt{2}\gamma b\xi$ by the operator $T_\lambda = -i\sqrt{2}\gamma b [\xi \cos(\lambda/2) - \eta \sin(\lambda/2)]$. In absence of phonon-electron interaction the electric current is given by³⁰

$$I = G_0 \int d\omega (n_L - n_R)D(\omega), \quad (7)$$

where $G_0 = 2e^2/h$ is the conductance quantum, $n_{L,R}$ are the Fermi distribution functions in the respective electrode and

$$D(\omega) = \frac{\omega^2\Gamma^2}{(\omega^2 - \Delta^2)^2 + \omega^2\Gamma^2} \quad (8)$$

is an effective transmission coefficient for the new fermions. Its nonmonotonic behavior around $\omega = 0$ for zero and finite Δ is the reason for the full transmission suppression in the off-resonant case²²⁻²⁴. The system under consideration is not the only one with the effective transmission coefficient of the form (8). It is also encountered in the exact analytic solution of the two-terminal Kondo model at the Toulouse point³¹ as well as in the transmission coefficient for the physical electrons in the parallel double quantum dot setup^{32,33}. The generalization of the phenomena discussed below to these setups is thus straightforward.

The cumulant generating function (CGF) for the system at $g \neq 0$ factorizes as $\chi(\lambda) = \chi_0(\lambda)\chi_g(\lambda)$, where $\chi_0(\lambda)$ is the CGF calculated in [27-29]. The correction due to electron-phonon coupling is found from

$$\ln \chi_g(\lambda) = \left\langle e^{-g \int_C d\tau [c^\dagger(\tau) + c(\tau)]a(\tau)b(\tau)} \right\rangle_\lambda \quad (9)$$

where the expectation value is taken with respect to the operator $H_0[\xi, \eta] - i\Delta ab + \Omega c^\dagger c + T_\lambda$. The time integration runs along the full Keldysh contour \mathcal{C} and the superscripts $k, l = \pm$ refer to the backward/forward propagating branches. In the leading order perturbation theory there are two different contributions: (i) the one generated by the ‘tadpole’ diagram

$$\ln \chi_{g,1}^{(1)} = -i\frac{g^2}{2} \sum_{k,l=\pm} (kl) \int_C d\tau_1 d\tau_2 G_{ph}^{kl}(\tau_{12}) \times \lim_{\epsilon \searrow 0} D_{ab}^{kk}(-k\epsilon) D_{ab}^{ll}(-l\epsilon); \quad (10)$$

(ii) the one given by the ‘shell’ diagram

$$\ln \chi_{g,2}^{(1)} = -i \frac{g^2}{2} \sum_{k,l=\pm} kl \int_{\mathcal{C}} d\tau_1 d\tau_2 G_{ph}^{kl}(\tau_{12}) \times \left[D_{ab}^{kl}(\tau_{12}) D_{ab}^{lk}(-\tau_{12}) - D_{aa}^{kl}(\tau_{12}) D_{bb}^{lk}(-\tau_{12}) \right]. \quad (11)$$

Here, we introduced the phonon Keldysh Green’s function (GF) $G_{ph}(\tau_{12}) = -i \langle T_{\mathcal{C}} c(\tau_1) c^\dagger(\tau_2) \rangle$, the Keldysh functions of the quantum dot $D_{\alpha\beta}(\tau_{12}) = -i \langle T_{\mathcal{C}} \alpha(\tau_1) \beta(\tau_2) \rangle_{\lambda}$ where α and β take values in the set $\{a, b\}$ and $\tau_{12} = \tau_1 - \tau_2$. At this point it is convenient to transform to energy variables

$$\ln \chi_{g,2}^{(1)} = \frac{g^2}{2} \sum_{k,l=\pm} (kl) \int \frac{d\omega}{2\pi} G_{ph}^{kl}(\omega) \pi^{kl}(\omega) \quad (12)$$

and introduce generalized (Keldysh) polarization loops

$$\pi^{kl}(\omega) = -i \int \frac{dy}{2\pi} \left[D_{ab}^{kl}(y+\omega) D_{ab}^{lk}(y) - D_{aa}^{kl}(y+\omega) D_{bb}^{lk}(y) \right] \quad (13)$$

In the resonant case ($\Delta = 0$) the mixed dot Keldysh GFs ($\alpha \neq \beta$) vanish identically and $D_{aa}(\omega)$ becomes diagonal. Hence, we are left with the calculation of the (anti-)time-ordered components of the polarization loop. In the zero temperature limit the first order correction to the full counting statistics can be calculated exactly. One finds

$$\ln \chi_g^{(1)} = -\frac{\mathcal{T} g^2 e^{i\frac{\Delta}{2}} \Gamma \tan^{-1}\left(\frac{V}{\Gamma} e^{-i\frac{\Delta}{2}}\right) - \Omega \tanh^{-1}\left(\frac{V}{\Omega}\right)}{2\pi (\Gamma^2 + \Omega^2 + \Gamma^2 (e^{i\lambda} - 1))}$$

Thus the correction to the transport current has the following form,

$$I^{(1)} = \frac{g^2}{2\pi} \Gamma^2 \left[\frac{V}{(V^2 + \Gamma^2)(\Gamma^2 + \Omega^2)} + \frac{(\Gamma^2 - \Omega^2) \tan^{-1}(V/\Gamma) - 2\Gamma\Omega \tanh^{-1}(V/\Omega)}{\Gamma(\Gamma^2 + \Omega^2)^2} \right] \quad (14)$$

Expressions for noise and higher cumulants can easily be determined by taking higher order derivatives of the CGF with respect to λ and setting it to zero afterwards. The calculation of the correction to the full statistics at finite temperature is quite involved. It is, in fact, more convenient to set up explicit expressions for the individual cumulants before the energy integration. A remarkable property is the absence of any sharp energy threshold usually found in phonon affected transport between uncorrelated electrodes. Those are usually attributed to the onset of inelastic processes^{11–13}, when individual electrons may loose/gain energy Ω during tunneling between the leads at $V \geq \Omega$. In the present case of MRLM the situation is different. The Majorana fermions describe the

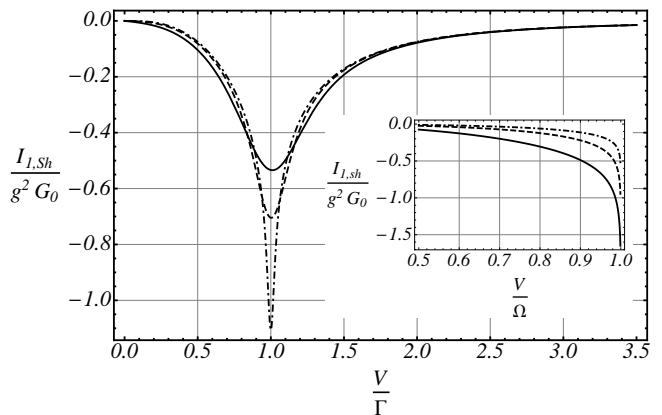


FIG. 1: *Main graph*: first order current correction at finite temperature. The parameters are $\Omega/\Gamma = 1$ and $T/\Gamma = 0.1, 0.05, 0.01$ (solid, dashed, dashed-dotted). *Inset*: first order current corrections in case of zero temperature for $\Omega/\Gamma = 1, 2, 3$ (solid, dashed, dashed-dotted)

collective excitations of the TLL state in the leads (kinks and antikinks), rather than individual electrons. That is why even at $T = 0$ there is no sharp energy threshold. Another feature is the logarithmic divergency for $V \rightarrow \Omega$, which does not survive at finite temperatures, see Fig. 1. It can be attributed to the non-monotonic behavior of the effective transmission coefficient (8) at zero and finite off-set Δ . The transmission for the quasiparticles drops immediately to zero as soon as Δ becomes off-resonant. This is exactly what occurs when the harmonic degree of freedom is excited – the coupling g generates an effective non-zero offset. In this voltage regime the problem becomes non-perturbative in the electron-phonon coupling and therefore requires analysis by more advanced methods. One possible route would be an RPA-like diagram resummation. To perform this program, we express the CGF in terms of the adiabatic potential³⁴, which itself can be rewritten as a function of the exact D_{bb} Keldysh GF only. It is approximated by the RPA-type summation (see Fig. 2 for the diagrammatic structure). Interestingly, within this approximation one finds

$$\begin{aligned} \overline{D_{bb}^{\text{RPA}}} = & \overline{D_{bb}} + \overline{D_{bb} \text{---} D_{aa} \text{---} D_{bb}} + \dots \\ & + \overline{D_{bb} \text{---} D_{aa} \text{---} D_{bb} \text{---} D_{aa} \text{---} D_{bb}} + \dots \end{aligned}$$

FIG. 2: Summation of an infinite series of diagrams. D_{bb} , D_{aa} represents the Keldyshfunction of the b resp. a Majorana fermions as defined before with λ set so zero and the wiggly lines represent the phonon propagators

for the CGF the Levitov-Lesovik formula³⁵

$$\ln \chi^{\text{RPA}}(\lambda) = \mathcal{T} \int \frac{d\omega}{2\pi} \ln [1 + D_0^{\text{eff}}(\omega) (e^{i\lambda} - 1) (n_L - n_R)] \quad (15)$$

with the effective transmission coefficient

$$D_0^{\text{eff}}(\omega) = \frac{\Gamma^2 (\omega^2 - \Omega^2)^2}{g^4 \omega^2 - 2g^2 \omega^2 (\omega^2 - \Omega^2) + (\omega^2 + \Gamma^2) (\omega^2 - \Omega^2)^2} \quad (16)$$

which has a three maxima (perfect transmission) at $\omega = 0, \pm\sqrt{g^2 + \Omega^2}$ and minima (perfect reflection) at $\omega = \pm\Omega$.

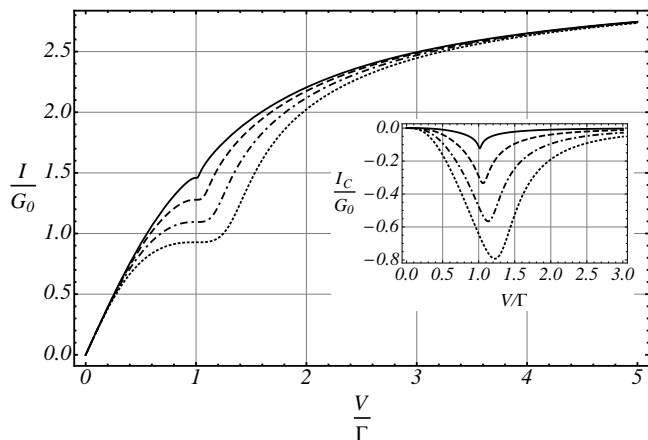


FIG. 3: *Main graph*: Full current in RPA approximation. The parameters are $\Omega/\Gamma = 1$ and $g/\Gamma = 0.25, 0.5, 0.75, 1$ (solid, dashed, dashed-dotted, dotted lines, respectively). *Inset*: the current correction in RPA approximation $\Omega/\Gamma = 1$ and $g/\Gamma = 0.25, 0.5, 0.75, 1$ (solid, dashed, dashed-dotted and dotted lines)

In Figs. 3 and 5 the current and noise in our approximation are depicted. One observes that for small voltages the current increases nearly linear. For voltages near Ω one finds a plateau, e. g. the current enhancement is suppressed by the electron-phonon interaction. This feature does not occur exactly at $V = \Omega$ (see Fig. 3). One finds that the maximal reduction of the current is at $V = \Omega\sqrt{1 + \frac{g^2}{2\Omega^2}}$ or if one assumes $\Omega \gg g$, $V \approx \Omega + \frac{1}{4}\frac{g^2}{\Omega}$. This kind of a shift by $\frac{g^2}{\Omega}$ is one normally produced by a polaron (Lang-Firsov) transformation¹⁸.

The behavior of the shot noise turns out to be even more interesting, see Fig. 4. In case of zero temperature, to the lowest order in g one again finds a log-divergent contribution for voltages approaching the phonon frequency. However, for a special configuration $\Gamma = \Omega$ the singularity cancels out and the shot noise interpolates in a regular way between small and large voltage limits. For $\Omega > \Gamma$ the correction to the shot noise develops a new feature: it changes sign, see Fig. 4 inset. Just as in the case of the transport current, the resummation heals the singularity, see Fig. 5.

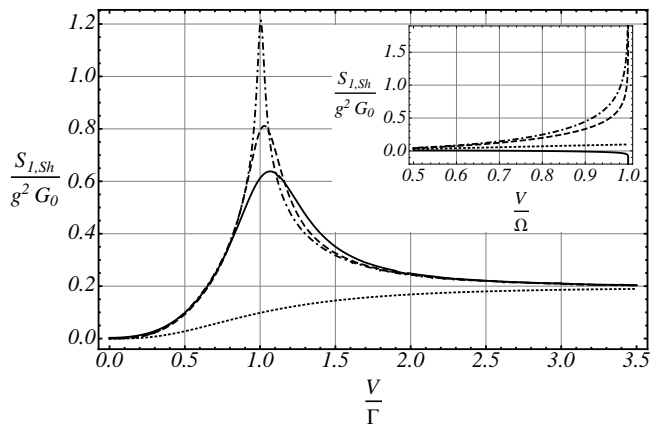


FIG. 4: *Main graph*: g^2 correction to the shot noise at finite temperatures. The plotting parameters are $\Omega/\Gamma = 1$ and $T/\Gamma = 0.1, 0.05, 0.01, 0$ (solid, dashed, dashed-dotted, dotted lines respectively). *Inset*: g^2 noise corrections in case of zero temperature. The plotting parameters are $\Gamma/\Omega = 1, 2, 3$ (solid, dashed, dashed-dotted lines)

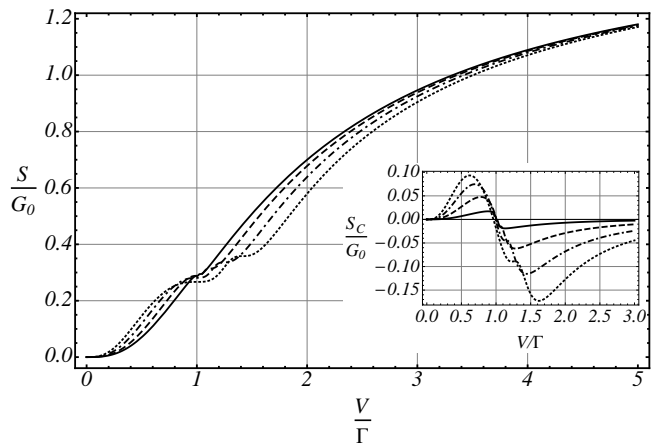


FIG. 5: *Main graph*: Shot noise in RPA approximation. The parameters are $\Omega/\Gamma = 1$ and $g/\Gamma = 0.25, 0.5, 0.75, 1$ (solid, dashed, dashed-dotted and dotted lines). *Inset*: noise correction in RPA approximation for $\Omega/\Gamma = 1$ and $g/\Gamma = 0.25, 0.5, 0.75, 1$ (solid, dashed, dashed-dotted and dotted lines).

There is an important difference in the behavior of the noise and current corrections in the high voltage limit. While the latter tends to vanish the former remains finite. It can be understood as follows. As already discussed in the introduction, for the current only the overall spectral density between the chemical potentials in the leads is essential. For $V \gg \Omega$ the phonon excitations are less effective in squeezing the spectral weight beyond the voltage window, so the current should approach the unitary value already in the zeroth order in g . For the noise, however, the rate of phonon (de)excitation is important. In the limit $V \rightarrow \infty$ it achieves its maximal value, thereby generating a finite contribution seen in Fig. 4. However, this feature isn't observed after the diagram subsuma-

tion procedure.

We now turn to the off-resonant system $\Delta \neq 0$. It is again convenient to perform the λ differentiations first and integrate over energy afterwards. Here two different regimes of weak $|\Delta| < \Gamma/2$ and strong detuning $|\Delta| > \Gamma/2$ emerge.^{22,26}

In the following we consider the case of weak detuning. Then, the tadpole contribution yields

$$I_{\text{tadpole}}^{(1)} = \frac{\Gamma\Delta}{2\pi\Omega} \frac{\ln\left(\frac{V^2+\Omega_+^2}{V^2+\Omega_-^2}\right)}{\Omega_-^2 - \Omega_+^2} \partial_\Delta \sum_{\pm} \frac{\pm\Gamma^2\Omega_{\pm} \tan^{-1}\left(\frac{V}{\Omega_{\pm}}\right)}{\Omega_+^2 - \Omega_-^2} \quad (17)$$

where we have defined $\Omega_{\pm} = \Gamma/2 \pm \sqrt{(\Gamma^2/4 - \Delta^2)}$. The

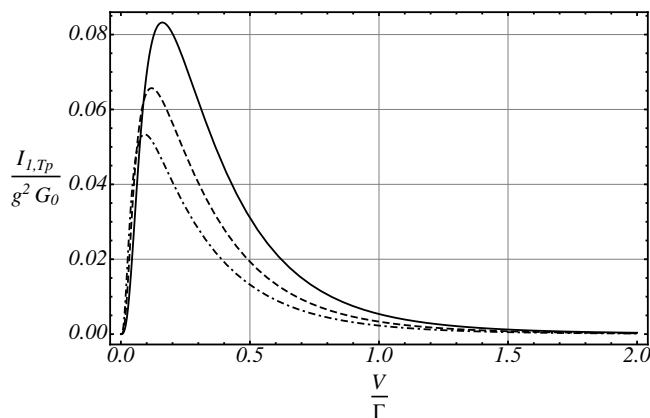


FIG. 6: Tadpole correction to the current. The parameters of the plots are $\Omega/\Gamma = 10$ and Δ/Γ takes the values 0.25, 0.2, 0.17 (solid, dashed and dot-dashed lines, respectively)

corresponding current correction is plotted in Fig. 6. Just as in the case of transport between two uncorrelated electrodes¹², its simple functional dependence on the phonon frequency hints at its dominance in the (Born-Oppenheimer) limit of the very ‘slow’ phonon^{36,37}. The parameter Γ mainly determines the width of the peak and Δ its position. Because of the simple form of this contribution, we will omit it in further illustrations.

The contributions from the shell diagram are more sophisticated:

$$I_{\text{shell}}^{(1)} = \frac{(g\Gamma)^2}{2} \int_{-V}^V \frac{dy}{2\pi} [j_1(y) + j_2(y) + j_3(y)], \quad (18)$$

where we have

$$j_1(y) = - \sum_{\pm} \frac{\Delta^2 (y^2 - \Delta^2)^2 y^2 + (y \pm \Omega)^2 + 2y(y \pm \Omega)}{D_0^2(y) D_0(y \pm \Omega)} \times [1 + \Theta(-V - y \mp \Omega)]$$

$$j_2(y) = - \sum_{\pm} \left[\frac{y\Delta^2 (\Delta^2 - (y \pm \Omega)^2) + y\Gamma^2 (y \pm \Omega)}{D_0(y \pm \Omega)} + \frac{(y^2 + \Delta^2)(y \pm \Omega) [(y + \Omega)^2 - \Delta^2]}{D_0(y \pm \Omega)} \right] \frac{y(y^2 - \Delta^2)}{D_0^2(y)},$$

where $D_0(y) = (y^2 - \Delta^2)^2 + y^2\Gamma^2$. The expression von j_3 is quite lengthy, see Appendix for details. Similar to the tadpole contribution this part is also always positive. In contrast to the resonant case, the corrections remain finite for every voltage. For V close to the phonon frequency we observe a double step like feature instead. This can be attributed to the double-maximum behavior of the transmission coefficient (8), the denominator $D_0(y)$ of which enters all relevant Green’s functions and thereby affects the voltage dependence. The linear scaling of the distance between the dips is shown in Fig. 7.

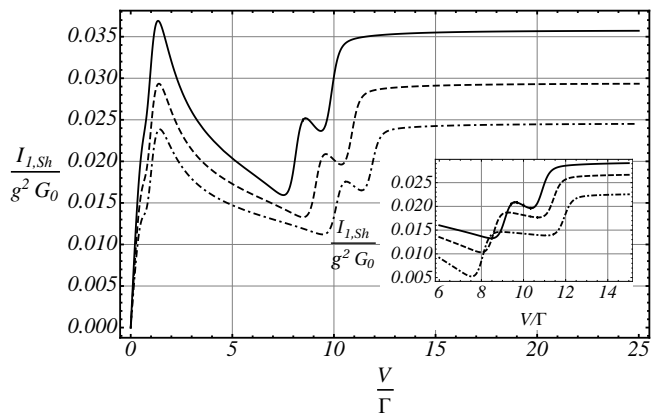


FIG. 7: *Main graph*: shell diagram correction to the current. The parameters of the plots are $\Delta/\Gamma = 1$ and Ω/Γ takes the values 9, 10, 11 (solid, dashed, dashed-dotted). *Inset*: double step like feature for the parameters $\Omega/\Gamma = 10$ and $\Delta/\Gamma = 1, 1.5, 2$ (solid, dashed, dashed-dotted). In both, the main graph and the inset, we chose strong detuning, because in this limit electron-phonon interaction effects are more pronounced.

To conclude, we investigated the interacting resonant level model in presence of a harmonic degree of freedom coupled to the quantum dot. We observe that in the resonant case, where the system is initially perfectly transmitting, finite electron-phonon coupling leads to negative corrections to the current. In the zero temperature limit we identified a strongly non-perturbative regime where the current correction is log-divergent and performed an RPA-like resummation of divergent diagram contributions, which turned out to produce a plateau-like feature in the full current-voltage characteristics of the system. We believe that this behaviour is generic in all setups with TLL electrodes also beyond the chosen parameter constellation. Single wall carbon nanotubes (SWNTs) are known to be typical realizations of the TLL electronic state.^{38–41} Therefore we expect the above strong conductance suppression phenomenon to be observable in exper-

iments on molecular quantum dots coupled to SWNTs. In the opposite off-resonant case, when the system without the phonon has zero conductance, we observe conductance enhancement due to electron-phonon interaction. For voltages comparable to phonon frequency we find a double-step like feature in the lowest order perturbation expansion in electron-phonon coupling. Contrary to the resonant case no singularities are observed.

The authors would like to thank T. L. Schmidt for many interesting discussions. The financial support was provided by the DFG under grant No. KO 2235/3 and by the Kompetenznetz ‘‘Funktionelle Nanostrukturen III’’ of the Baden-Württemberg Stiftung (Germany).

Appendix A: Tadpole contribution in case of strong detuning

In case of strong detuning $\Delta^2 > \frac{\Gamma^2}{4}$ one finds for the static contribution the expression

$$I_{\text{static}} = \frac{4}{\pi\Omega} \sum_{\pm} \frac{\tanh^{-1} \left[\frac{\pm 2V - \Gamma}{\sqrt{4\Delta^2 - \Gamma^2}} \right]}{\sqrt{4\Delta^2 - \Gamma^2}} \quad (\text{A1})$$

$$\times \partial_{\Gamma} \left[\frac{\sum_{\pm} \pm \tanh^{-1} \left[\frac{\pm 2V - \Gamma}{\sqrt{4\Delta^2 - \Gamma^2}} \right]}{\sqrt{4\Delta^2 - \Gamma^2}} \right]. \quad (\text{A2})$$

Appendix B: Explicit expression of the j_3 current contribution

With the definitions

$$\begin{aligned} f_{rp} &:= (\omega + r\Omega)^2 - r\Omega_p^2 \\ g_p &:= \Omega^4 + 2\Omega^2(\Omega_p^2 - \omega^2) + (\omega^2 + \Omega_p^2)^2 \\ h_r &:= \ln \frac{(\omega - r\Omega)^2 - V^2}{\Gamma^2} \\ k_p &:= \ln \frac{V^2 + \Omega_p^2}{\Gamma^2} \end{aligned}$$

where the indices r, p run over $\{\pm\}$ together with

$$\begin{aligned} h_1 &= \sum_{r,p=\pm} \left[\frac{\pi p \Omega (\omega^2 - \Omega^2 + \Omega_+ \Omega_-)}{|\Omega_p| \left[\Omega^2 + (i\omega + \Omega_+)^2 \right] \left[\Omega^2 + (i\omega + \Omega_-)^2 \right]} \right. \\ &\quad \left. + \frac{p f_{rp} h_r + \omega \Omega k_p}{g_p} + \frac{\pi p \Omega |\Omega_p| (\Omega^2 - \omega^2 + \Omega_p^2)}{g_p} \right] \\ h_2 &= \sum_{r,p=\pm} \left[\frac{i \pi p \Omega \Omega_p (i\omega + \Omega_p)}{\left[\Omega^2 + (i\omega + \Omega_+)^2 \right] \left[\Omega^2 + (i\omega + \Omega_-)^2 \right]} \right. \\ &\quad \left. + \frac{1}{2} \frac{\pi |\Omega_p|}{(\omega - \Omega)^2 + \Omega_p^2} + \frac{(\omega + r\Omega)(h_r + r k_p)}{\left[(\omega - r\Omega)^2 + \Omega_p^2 \right]} \right] \frac{4}{\Omega_+^2 - \Omega_-^2} \\ h_3 &= \sum_{p=\pm} \left[\frac{-2\pi p \Omega (\Omega^2 - \omega^2 + \Omega_p^2)}{|\Omega_p| g_p (\Omega_+^2 - \Omega_-^2)} + \frac{p f_{p+} f_{p-} h_p}{g_+ g_-} \right. \\ &\quad \left. - \frac{p \omega \Omega k_p}{g_p (\Omega_+^2 - \Omega_-^2)} \right] \end{aligned}$$

one finds for j_3

$$j_3(\omega) = \frac{(\omega^2 - \Delta^2) \omega \Delta^2 \Gamma^3}{(4\pi) D_0(\omega)^2} \left[h_1(\omega) + \omega h_2(\omega) + \omega^2 h_3(\omega) \right] \quad (\text{B1})$$

¹ P. W. Anderson, Phys. Rev. **124**, 41 (1961).

² T. Holstein, Annals of Physics **8**, 325 (1959).

³ A. C. Hewson and D. Meyer, Journal of Physics: Condensed Matter **14**, 427 (2002).

⁴ N. B. Zhitenev, H. Meng, and Z. Bao, Phys. Rev. Lett. **88**, 226801 (2002).

⁵ X. H. Qiu, G. V. Nazin, and W. Ho, Phys. Rev. Lett. **92**, 206102 (2004).

⁶ L. H. Yu, Z. K. Keane, J. W. Ciszek, L. Cheng, M. P. Stewart, J. M. Tour, and D. Natelson, Phys. Rev. Lett. **93**, 266802 (2004).

⁷ A. N. Pasupathy, J. Park, C. Chang, A. V. Soldatov, S. Lebedkin, R. C. Bialczak, J. E. Grose, L. A. K. Donev, J. P. Sethna, D. C. Ralph, et al., Nano Lett. **5**, 203 (2005).

⁸ S. Sapmaz, P. Jarillo-Herrero, Y. M. Blanter, C. Dekker,

and H. S. J. van der Zant, Phys. Rev. Lett. **96**, 026801 (2006).

⁹ D. Djukic, K. S. Thygesen, C. Untiedt, R. H. M. Smit, K. W. Jacobsen, and J. M. van Ruitenbeek, Phys. Rev. B **71**, 161402(R) (2005).

¹⁰ R. H. M. Smit, Y. Noat, C. Untiedt, N. D. Lang, M. C. van Hemert, and J. M. van Ruitenbeek, Nature **419**, 906 (2002).

¹¹ R. Egger and A. O. Gogolin, Phys. Rev. B **77**, 113405 (2008).

¹² T. L. Schmidt and A. Komnik, Phys. Rev. B **80**, 041307 (pages 4) (2009).

¹³ L. de la Vega, A. Martín-Rodero, N. Agraït, and A. L. Yeyati, Phys. Rev. B **73**, 075428 (2006).

¹⁴ M. Paulsson, T. Frederiksen, and M. Brandbyge, Phys.

- Rev. B **72**, 201101 (2005).
- ¹⁵ T. Mii, S. G. Tikhodeev, and H. Ueba, Phys. Rev. B **68**, 205406 (2003).
 - ¹⁶ R. Avriller and A. Levy Yeyati, Phys. Rev. B **80**, 041309 (2009).
 - ¹⁷ F. Haupt, T. Novotný, and W. Belzig, Phys. Rev. Lett. **103**, 136601 (2009).
 - ¹⁸ G. Mahan, *Many-particle physics* (Plenum press, 1991).
 - ¹⁹ S. Braig and K. Flensberg, Phys. Rev. B **68**, 205324 (2003).
 - ²⁰ C. L. Kane and M. P. A. Fisher, Phys. Rev. B **46**, 15233 (1992).
 - ²¹ A. Furusaki and N. Nagaosa, Phys. Rev. B **47**, 4631 (1993).
 - ²² A. Komnik and A. O. Gogolin, Phys. Rev. Lett. **90**, 246403 (2003).
 - ²³ Y. V. Nazarov and L. I. Glazman, Phys. Rev. Lett. **91**, 126804 (2003).
 - ²⁴ D. G. Polyakov and I. V. Gornyi, Phys. Rev. B **68**, 035421 (2003).
 - ²⁵ A. Furusaki, Phys. Rev. B **57**, 7141 (1998).
 - ²⁶ A. Komnik, Phys. Rev. B **79**, 245102 (pages 5) (2009).
 - ²⁷ A. V. Andreev and E. G. Mishchenko, Phys. Rev. B **64**, 233316 (2001).
 - ²⁸ M. Kindermann and B. Trauzettel, Phys. Rev. Lett. **94**, 166803 (2005).
 - ²⁹ A. Komnik and A. O. Gogolin, Phys. Rev. Lett. **94**, 216601 (2005).
 - ³⁰ A. Komnik and A. O. Gogolin, Phys. Rev. B **68**, 235323 (2003).
 - ³¹ A. Schiller and S. Hershfield, Phys. Rev. B **58**, 14978 (1998).
 - ³² B. Kubala and J. König, Phys. Rev. B **67**, 205303 (2003).
 - ³³ J. P. Dahlhaus, S. Maier, and A. Komnik, Phys. Rev. B **81**, 075110 (2010).
 - ³⁴ A. O. Gogolin and A. Komnik, Phys. Rev. B **73**, 195301 (2006).
 - ³⁵ L. S. Levitov, W. W. Lee, and G. B. Lesovik, J. Math. Phys. **37**, 4845 (1996).
 - ³⁶ A. O. Gogolin and A. Komnik, cond-mat/0207513 (2002).
 - ³⁷ R.-P. Riwar and T. L. Schmidt, Phys. Rev. B **80**, 125109 (2009).
 - ³⁸ R. Egger and A. Gogolin, Phys. Rev. Lett. **79**, 5082 (1997).
 - ³⁹ C. Kane, L. Balents, and M. Fisher, Phys. Rev. B **79**, 5086 (1997).
 - ⁴⁰ M. Bockrath, D. H. Cobden, J. Lu, A. G. Rinzler, R. E. Smalley, L. Balents, and P. L. McEuen, Nature **397**, 598 (1999).
 - ⁴¹ Z. Yao, H. W. C. Postma, L. Balents, and C. Dekker, Nature **402**, 273 (1999).